ICT Express 12 (2026) 571–575

Contents lists available at ScienceDirect

ICT Express

journal homepage: www.elsevier.com/locate/icte

Connectivity and stability analysis for UAVs in urban networks

Sooyeob Jung [a], Pansoo Kim [b], Song Noh [c,*], Junse Lee [d,*]

[a] School of Information and Communication Engineering, Chungbuk National University, Cheongju 28644, Republic of Korea
[b] Satellite Wide-Area Infra Research Section, Electronics and Telecommunications Research Institute, Daejeon 34129, Republic of Korea
[c] Department of Information Telecommunication Engineering, Incheon National University, Incheon 22012, Republic of Korea
[d] School of AI Convergence, Sungshin Women's University, Seoul 02844, Republic of Korea

ARTICLE INFO

Keywords:
Unmanned Aerial Vehicles
Urban Outdoor Network
Stochastic geometry

ABSTRACT

Low-altitude UAVs are frequently blocked by obstacles (or buildings) in urban networks. So, the link stability is as critical as coverage probability. In this paper, we analyze the dynamic connectivity of a UAV-to-Ground link using stochastic geometry. We model buildings as a marked homogeneous Poisson Point Process. Using this model, we obtain analytical expressions for the mean total connection time and the expected number of interruptions. We reveal a fundamental trade-off between improving connection time and interruptions. We provide the existence of an optimal flight altitude numerically, which balances the connectivity and stability of a UAV-to-ground link.

1. Introduction

Unmanned Aerial Vehicles (UAVs) are creating new paradigms for ubiquitous 3D connectivity in 6G networks [1]. UAVs will act as base stations or relays and are expected to support diverse applications from urban air mobility (UAM) to disaster management. However, establishing reliable links in dense urban environments is challenging due to obstacles such as high-rise buildings. UAVs operate in a highly dynamic environment, unlike terrestrial networks, so robust link stability is required to maintain continuous control and data transmission.

Many statistical models have been proposed to characterize such blockage effects. For example, ray-tracing provides network analysis based on the phenomena of radio wave propagation. It provides site-specific accuracy but does not show the relationship between network performances and network parameters. In the meantime, stochastic geometry has been widely used to analyze the network performance by modeling network entities as random point processes [2]. This mathematical tool has been successfully applied to provide valuable insights for understanding cellular networks [3], ad-hoc networks [4]. Our recent work also utilized this framework to characterize sky visibility and line-of-sight (LoS) probability of ground users [5,6] by modeling obstacles (or buildings) as a marked homogeneous Poisson point process (PPP).

In previous works under the stochastic geometry framework, network performances are obtained by averaging over independent network snapshots, neglecting the kinematic features of the UAVs. Due to the mobility of UAVs, a link could suffer from rapid on–off switching, or, namely, flickering, caused by blockages, and a high average LoS probability cannot capture this phenomenon. This effect makes excessive signaling overhead and degrades the QoS of network services. So, a comprehensive analysis is required to understand the service duration and interruption rate for UAV networks jointly.

UAV connectivity in dynamic and complex scenarios has been researched. Zhao et al. [7] developed a multi-UAV collaboration task scheduling framework that facilitates reinforcement learning to maximize network performance in dynamic environments. In addition, improving the security and energy efficiency of UAV-enabled networks using reconfigurable intelligent surfaces (RISs) has been researched [8,9]. Furthermore, the methods for mounting and using RISs in UAVs for integrated sensing and communication (ISAC) systems have emerged as a key research area [10].

Although these studies provide important insights through optimization or AI-based approaches, they are characterized by a strong dependence on line-of-sight (LoS) links. The stochastic geometry-based framework proposed in this paper complements these prior studies by providing a fundamental analysis of link stability. The interruption rate derived in this study provides an important performance bound

* Corresponding authors.
E-mail addresses: syjung@chungbuk.ac.kr (S. Jung), pskim@etri.re.kr (P. Kim), songnoh@inu.ac.kr (S. Noh), junselee@sungshin.ac.kr (J. Lee).

https://doi.org/10.1016/j.icte.2026.02.011
Received 12 December 2025; Received in revised form 24 January 2026; Accepted 24 February 2026
Available online 27 February 2026
2405-9595/

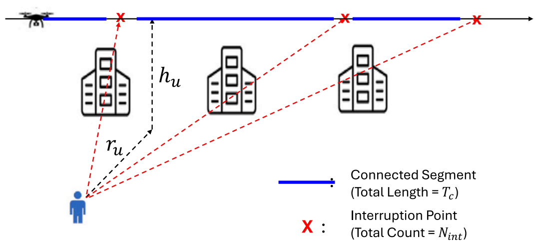

Fig. 1. System model of the UAV-to-Ground communication link. The UAV moves at a fixed altitude h_u with a horizontal offset r_u. The connectivity is determined by the blockage status along the LoS path.

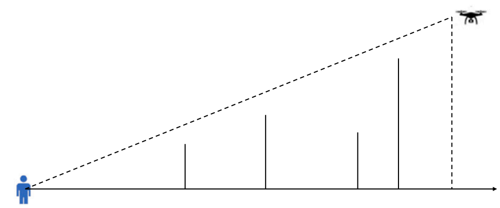

Fig. 2. Illustration of the blockage projection. The 2D building distribution (top) is projected onto the UAV's flight path direction, resulting in a 1D linear blockage process (bottom) with effective intensity λ.

for determining beamforming availability in RIS systems and sensing accuracy in ISAC scenarios.

In this paper, we propose an analytical framework to evaluate the dynamic connectivity of a UAV-to-Ground link using stochastic geometry. We model the locations of building as a homogeneous PPP. By leveraging the geometric properties of the blockage process along the UAV's trajectory, we extend the static analysis to a dynamic scenario. The main contributions are summarized as follows:

- We derive a closed-form expression of the LoS probability between a UAV and a ground user (Lemma 1). We model the blockage along the link projection as a 1D PPP. This derivation explicitly accounts for the UAV's finite altitude and the specific geometry of the link.
- Based on the result in Lemma 1, we provide analytical expressions of the expected total connection time and the expected number of interruptions in Theorems 1 and 2. These results provide the intuition on the link connectivity as functions of the UAV trajectory (r_u, h_u) and network parameters.
- Our numerical results reveal a fundamental trade-off: while increasing altitude improves connection time, it may degrade link stability due to the flickering effect. We demonstrate the existence of an optimal flight altitude that maximizes the effective throughput by balancing these conflicting objectives.

2. System model

2.1. Network geometry

We consider a dense urban environment where a UAV transmits data to a ground user located at the origin $(0,0,0) \in \mathbb{R}^3$. As illustrated in Fig. 1, the UAV moves along a linear trajectory at a constant velocity v at an altitude h_u. In a practical scenario, UAV operations involve acceleration and deceleration phases. However, we assume a constant velocity in this study since constant-speed trajectories are widely adopted to maximize energy efficiency and ensure uniform coverage in UAV operations [11,12]. We assume that the minimum horizontal offset distance of the UAV trajectory from the user is r_u. At time t, the distance between the user and UAV and elevation angle to the UAV observed by the user are denoted as $d(t)$ and $\theta(t)$. Then, $d(t)$ and $\theta(t)$ are given by:

$$d(t) = \sqrt{r_u^2 + (vt)^2 + h_u^2}, \tag{1}$$

$$\theta(t) = \arcsin\left(\frac{h_u}{d(t)}\right). \tag{2}$$

We also assume that UAV served reliable communication to the ground user when $d(t) \le d_{th}$, where d_{th} is the distance to serve the received Signal-to-Noise Ratio for a reliable communication. So, the effective service period is between $[-T_{max}(r_u, h_u), T_{max}(r_u, h_u)]$, where $T_{max}(r_u, h_u) = \frac{1}{v}\sqrt{d_{th}^2 - r_u^2 - h_u^2}$.

2.2. Stochastic blockage modeling

To characterize the blockages in the urban environment, we model the locations of buildings as a 2D homogeneous marked PPP, denoted by Φ_2, with a spatial density λ_2. Each building is modeled as a blockage obstacle with an average width $\bar{W}$ and a random height H following an exponential distribution with mean μ.

We simplify the blockage analysis by projecting the 2D building distribution onto the ground projection of the LoS link, as depicted in Fig. 2 for analytical tractability. This projection simplifies the analysis of the networks by transforming the 3D model into a 2D model, and we denote the location of blockages by Φ_1. So, buildings are treated as vertical line segments on the 1D path. Let λ be the effective linear intensity of Φ_1 and the relation of λ and λ_2 is

$$\lambda = \frac{2}{\pi}\lambda_2 \bar{W}. \tag{3}$$

While we acknowledge that blockage events are inherently spatially correlated as investigated in [13], incorporating such high-order statistics often leads to analytical intractability. Therefore, to obtain tractable closed-form expressions for the dynamic metrics, we focus on the first-order statistics by assuming that blockage events at distinct points along the trajectory are statistically independent [14]. Based on this 1D framework, we analyze the expected total connection time ($\bar{T}_{conn}$) and the expected number of interruptions ($\bar{N}_{int}$) over the effective service interval.

3. Dynamic connectivity analysis

In this section, we derive analytical expressions for the proposed dynamic metrics based on the stochastic geometry framework established in Section 2.

3.1. Instantaneous LoS probability

First, we derive the probability that the LoS link is unobstructed at a specific time instance t. Based on the 1D projection model illustrated in Fig. 2, the blockage status is determined by the buildings located along the ground projection of the link, denoted by the interval $[0, r(t)]$, where $r(t) = \sqrt{r_u^2 + (vt)^2}$ is the horizontal distance.

Lemma 1. *For a UAV at altitude h_u and horizontal distance $r(t)$, the instantaneous LoS probability is given by:*

$$P_{LoS}^{r_u,h_u}(t) = \exp\left(-\frac{\lambda\mu r(t)}{h_u}\left(1 - e^{-\frac{h_u}{\mu}}\right)\right), \tag{4}$$

where $\lambda = \frac{2}{\pi}\lambda_2\bar{W}$ is the effective 1D building density.

Proof. Let us consider a building located at a distance x between the ground user and the UAV at an altitude h_u and a horizontal distance $r(t)$. If its height H is larger than $L(x) = \frac{h_u}{r(t)}x$, the building makes this link NLoS (Non-Line-of-Sight), and the probability that this building blocks the link is $\mathbb{P}[H > L(x)] = \exp(-\frac{h_u x}{r(t)\mu})$.

So, we can conclude that the locations of blocking building form an inhomogeneous marked PPP with intensity $\lambda \exp(-\frac{h_u x}{r(t)\mu})$. So, the mean number of blocking buildings is obtained by integrating this intensity over the path:

$$\Lambda_{block}^{r_u,h_u} = \int_0^{r(t)} \lambda \exp\left(-\frac{h_u x}{r(t)\mu}\right) dx = \frac{\lambda \mu r(t)}{h_u}\left(1 - e^{-\frac{h_u}{\mu}}\right). \tag{5}$$

The LoS probability is the void probability that no blocking buildings exist, i.e., $P_{LoS}^{r_u,h_u}(t) = \exp(-\Lambda_{block}^{r_u,h_u})$, which completes the proof.

Remark (Urban Canyon Effect): Our model captures the severe shadowing effects of dense urban environments. At low altitudes, the derived blockage probability approaches unity due to the high obstacle density (λ). This is aligned with the deep shadowing observed in physical urban canyons.

3.2. Expected total connection time

The expected total connection time represents the accumulated duration during which the link remains in the LoS state. This is obtained by integrating the instantaneous LoS probability derived in Lemma 1 over the effective service interval.

We define $\bar{T}_{conn}(r_u, h_u)$ as the summation of connected time where the link between the ground user and UAV on the trajectory (r_u, h_u) remains as the LoS state. This metric is the aggregated service time of all fragmented LoS intervals. This metric is highly related to the delay-tolerant applications, such as sensor data collection and bulk file transfer, where the total size of transferred data depends on the total service time rather than the link continuity.

Based on Lemma 1, the expected total connection time is obtained by integrating the instantaneous LoS probability.

Theorem 1. *The mean value of total connection time is*

$$\mathbb{E}[\bar{T}_{conn}(r_u, h_u)] = 2\int_0^{T_{max}(r_u,h_u)} P_{LoS}^{r_u,h_u}(t)\, dt, \tag{6}$$

for given r_u and h_u.

Substituting (4) into the integral yields a closed-form expression involving the geometric parameters. Note that increasing h_u has a dual effect: it increases $P_{LoS}^{r_u,h_u}(t)$ (improving connectivity) but decreases $T_{max}(r_u, h_u)$ (reducing coverage range due to path loss), suggesting a trade-off.

3.3. Expected number of interruptions

In the previous subsection, we presented the total connection time, which can be used to quantify service volume. However, this metric cannot measure the detrimental frequent on–off switching, which reflects link stability. We define the expected number of interruptions, $\bar{N}_{int}$, to analyze the link stability, which is the accumulated rate of transitions from LoS to NLoS states over the flight path.

Remark 1 (*Independence Assumption*).
The aggregate blockage effect, which determines the LoS probability (P_{LoS}) and the local boundary crossing event causing interruptions, originates from the same underlying building process Φ. However, we invoke the fundamental property of the PPP where the number of points falling in disjoint spatial sets is statistically independent. The condition that the current link is LoS implies that the spatial region corresponding to the link is void of obstacles. Conversely, the interruption event occurs when the UAV encounters a new obstacle along the incremental flight path. We treat them as independent of each other since these two events pertain to non-overlapping spatial volumes. This assumption enables the derivation of tractable, closed-form analysis.

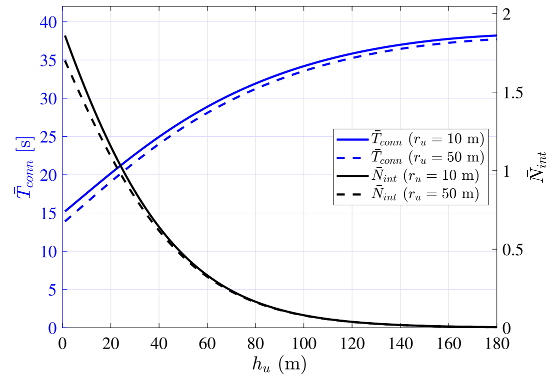

Fig. 3. Performance trade-off analysis with varying horizontal offsets (r_u). The blue lines represent the connection time ($\bar{T}_{conn}$), and the black lines represent the interruption rate ($\bar{N}_{int}$). Solid lines denote the near-user case ($r_u = 10$ m), while dashed lines denote the far-user case ($r_u = 50$ m). Note that the peak of instability (black) shifts to higher altitudes as r_u increases.

Theorem 2. *The expected number of interruptions is given by:*

$$\mathbb{E}[\bar{N}_{int}(r_u, h_u)] = 2\int_0^{T_{max}(r_u,h_u)} \lambda v \cdot e^{-\frac{h_u}{\mu}} \cdot P_{LoS}^{r_u,h_u}(t)\, dt. \tag{7}$$

Proof. We identify the condition for a transition from a LoS to an NLoS state. This transition occurs only when the UAV, moving at velocity v, physically enters the shadow of a building while the link is currently active.

First, consider the blockage caused by buildings near the ground user. These obstacles generally result in static blockage zones. If such a building blocks the link, the instantaneous probability $P_{LoS}^{r_u,h_u}(t)$ becomes zero. In this case, the link is already broken, and thus no new interruption event can be triggered. This user-perspective blockage is fully captured by the $P_{LoS}^{r_u,h_u}(t)$ term.

Second, dynamic interruptions are driven by the UAV's traversal across building boundaries. UAV moves along a trajectory with a constant altitude h_u. The connection state of link from UAV to the ground user changes from LoS to NLoS when the encountering building height is larger than h_u, and its probability is $\mathbb{P}[H > h_u] = e^{-h_u/\mu}$.

So, we can conclude that $\mathbb{E}[\bar{N}_{int}(r_u, h_u)]$ is the product of λv, the conditional blockage probability $e^{-h_u/\mu}$, and the link availability $P_{LoS}^{r_u,h_u}(t)$.

4. Numerical results

We evaluate the dynamic connectivity performance of the UAV-to-Ground link based on the analytical framework derived in Section 3.

4.1. Simulation setup

The urban environment is modeled as a PPP with a building density of $\lambda_2 = 500$ buildings/km^2. The buildings have an average width of $\bar{W} = 20$ m and their heights follow an exponential distribution with a mean of $\mu = 25$ m. Based on the projection model in Section 2, the effective 1D linear density is $\lambda = \frac{2}{\pi}\lambda_2 \bar{W} \approx 6.36$ buildings/km. The UAV flies at a constant velocity of $v = 20$ m/s. The threshold distance is set to $d_{th} = 500$ m. We obtained this value from the maximum effective communication range under a standard path loss model where a path loss exponent of $\alpha = 3.5$, a transmit power of $P_{tx} = 23$ dBm, and a noise floor of -100 dBm. We investigate the impact of the horizontal geometry by comparing two scenarios: a near-user path ($r_u = 10$ m) and a far-user path ($r_u = 50$ m).

Remark (Impact of Building Density): For the numerical results, we present only the case of $\lambda = 500$ (typically in high-density urban areas). As shown in (6) and (7), the building density λ acts as a scaling factor for the blocking parameter β. As a result, the shape of the curve remains consistent even in lower or higher λ, but only shifts in optimal elevation. In other words, higher densities require higher flight altitudes to obtain the same LoS probability.

4.2. Performance analysis

Fig. 3 illustrates the fundamental trade-off between the expected total connection time ($\bar{T}_{conn}$) and the expected number of interruptions ($\bar{N}_{int}$) with respect to the flight altitude h_u.

4.2.1. Connection time

The expected total connection time ($\bar{T}_{conn}$) generally improves as the UAV altitude increases, as a higher elevation angle reduces the blockage probability.

- For the near-user case ($r_u = 10$ m), the connection time rises rapidly even at low altitudes ($h_u < 50$ m) because the UAV is almost directly above the user, minimizing blockage effects.
- In contrast, for the far-user case ($r_u = 50$ m), the UAV should fly higher altitude to clear the obstacles. Furthermore, as h_u exceeds a certain limit ($h_u > 120$ m), $\bar{T}_{conn}$ drops sharply. This is because the UAV reaches the maximum path loss distance (d_{th}), causing the effective service interval T_{max} to shrink. This drop occurs earlier for the far-user case since the horizontal offset consumes a portion of the link budget.
- Effect of Horizontal Distance: We also analyze the impact of the horizontal distance r_u on the connection time. As r_u increases, the angle of elevation between the user and the UAV inevitably decreases. This geometric change greatly increases the probability of blockage by the building, which in turn leads to a decrease in the average total connection time. Therefore, UAVs must operate at higher elevations to maintain the same level of connectivity at greater distances. This physical constraint explains the rightward shift of the optimal altitude observed in the results as r_u increases.

4.2.2. Interruption rate

The expected number of interruptions ($\bar{N}_{int}$) exhibits a distinct unimodal behavior, revealing the flickering effect.

- At low altitudes (e.g., $h_u < 10$ m), the link is likely blocked, and it results few interruptions.
- As h_u increases to moderate altitudes, the interruption rate shoots up, creating a peak region. This corresponds to the altitude where the UAV flight path intersects the highest density of building rooftops, causing rapid on–off switching.
- Notably, the peak of the interruption rate shifts to the right as r_u increases (from $h_u \approx 25$ m for $r_u = 10$ m to $h_u \approx 60$ m for $r_u = 50$ m). This implies that when the UAV is horizontally further away, the unstable zone occurs at higher altitudes due to the lower elevation angle.
- We observe the relationship between the interruption rate and altitude. At low altitudes, the link is blocked by buildings, which leads to a constant blocked state rather than frequent switching. Thus, the interruption rate is relatively low, but the connection time is minimal. As the UAV rises to medium altitudes (Flickering Zone), the LoS probability improves, but the link frequently intersects with buildings. This creates a flickering effect, causing the interruption rate to reach its peak (worst stability). Finally, at high altitudes (LoS Dominance), once the UAV clears the average building height, the LoS link becomes dominant, and the interruption rate drops significantly, approaching zero.

Insight and Application Scenarios: We can obtain a clear network design trade-off by observing the crossing behavior of the two metrics. To achieve robust connectivity, the UAV must fly at an altitude sufficiently higher than the flickering peak to ensure link stability, yet lower than the SNR cutoff to maintain service availability. Consequently, a feasible operational altitude window exists, which becomes narrower and shifts to higher altitudes as the horizontal offset r_u increases.

The primary goal of services such as large-file transfers or sensor data collection is to maximize the total amount of data transferred. For delay-tolerant applications such as bulk file transfer or sensor data gathering, the primary goal is to maximize the total data volume. So, it is important to maximize the Total Connection Time ($\bar{T}_{conn}$). For delay-sensitive applications such as real-time video streaming, UAM control links, or URLLC, it is important to increase the link stability since frequent on–off switching (flickering) can cause synchronization loss or control failure. Therefore, minimizing the interruption rate ($\bar{N}_{int}$) is essential.

5. Conclusion

In this paper, we investigated the dynamic connectivity of UAV-to-Ground links in dense urban networks. We modeled the location of buildings as a homogeneous PPP. We derived two key kinematic metrics (the expected total connection time and the expected number of interruptions) in closed form.

We observed a numerical relationship between connection time and link stability. While higher altitude improves the connection duration, it induces a flickering effect, leading to a sharp peak in the interruption rate. We also observed that the horizontal offset (r_u) significantly influences this trade-off.

Our results show that simply increasing altitude for LoS connection is not an optimal solution. There exists an optimal altitude that balances service time and link stability.

CRediT authorship contribution statement

Sooyeob Jung: Writing – original draft, Formal analysis. **Pansoo Kim:** Writing – review & editing, Writing – original draft, Formal analysis. **Song Noh:** Writing – review & editing, Writing – original draft, Formal analysis, Conceptualization. **Junse Lee:** Writing – review & editing, Writing – original draft, Validation, Formal analysis, Conceptualization.

Declaration of competing interest

The authors have declared no conflict of interest.

Acknowledgments

This work was supported by the Institute of Information & communications Technology Planning & Evaluation (IITP) grant funded by the Korean government (MSIT) (RS-2024-00348050, Development of core technology of user terminal for low orbit satellite communication based on 3GPP standards).

References

[1] G. Araniti, A. Iera, S. Pizzi, F. Rinaldi, Toward 6G non-terrestrial networks, IEEE Netw. 36 (1) (2021) 113–120, http://dx.doi.org/10.1109/MNET.011.2100191.

[2] F. Baccelli, B. Błaszczyszyn, Stochastic geometry and wireless networks, in: Volume I - Theory, Now Publishers, Inc, 2009.

[3] J.G. Andrews, F. Baccelli, R.K. Ganti, A tractable approach to coverage and rate in cellular networks, IEEE Trans. Commun. 59 (11) (2011) 3122–3134, http://dx.doi.org/10.1109/TCOMM.2011.100411.100541.

[4] F. Baccelli, B. Bł aszczyszyn, P. Muhlethaler, An aloha protocol for multihop mobile wireless networks, IEEE Trans. Inform. Theory 52 (2) (2006) 421–436, http://dx.doi.org/10.1109/TIT.2005.862098.

[5] H. Yu, S. Jung, J. Ryu, J. Lee, Sky visibility under urban networks: A stochastic geometry approach, ICT Express 11 (1) (2025) 157–160, http://dx.doi.org/10.1016/j.icte.2024.12.002.

[6] J. Lee, F. Baccelli, How much can reconfigurable intelligent surfaces augment sky visibility: A stochastic geometry approach, IEEE Trans. Wirel. Commun. 24 (1) (2025) 796–809, http://dx.doi.org/10.1109/TWC.2024.3501953.

[7] L. Zhao, S. Li, Z. Tan, A. Hawbani, S. Timotheou, K. Yu, A multi-UAV cooperative task scheduling in dynamic environments: Throughput maximization, IEEE Trans. Comput. 74 (2) (2025) 442–454, http://dx.doi.org/10.1109/TC.2024.3483636.

[8] D. Wang, T. Liu, L. Li, W. Yang, Y. Jin, H. Zhao, Y. He, R. Zhang, Performance analysis of UAV–RIS-assisted short-packet secure communications, IEEE Internet Things J. 12 (24) (2025) 53039–53054, http://dx.doi.org/10.1109/JIOT.2025.3616305.

[9] J. Li, D. Wang, H. Zhao, Y. Jin, Y. He, F. Zhou, Z. Wei, V.C.M. Leung, Enhancing secrecy energy efficiency in UAV-ris assisted mobile IoV networks through DRL, IEEE Trans. Wirel. Commun. 25 (2025) 2092–2108, http://dx.doi.org/10.1109/TWC.2025.3594691.

[10] Y. Liu, D. Wang, H. Feng, Y. Jin, L. Pang, W. Yang, L. Li, Energy efficiency optimization for UAV-mounted RIS-aided integrated sensing and communication systems, Chin. J. Aeronaut. (2025) http://dx.doi.org/10.1016/j.cja.2025.103920.

[11] P. Panyakeow, M. Mesbahi, Deconfliction algorithms for a pair of constant speed unmanned aerial vehicles, IEEE Trans. Aerosp. Electron. Syst. 50 (1) (2014) 456–476, http://dx.doi.org/10.1109/TAES.2013.110766.

[12] M. Malekzadeh, A. Ghasemi, H. Pishro-Nik, Constant-speed trajectory processes for uniform coverage in UAV networks, in: Proc. 59th Annu. Conf. Inf. Sci. Syst., CISS, 2025.

[13] J. Lee, F. Baccelli, On the effect of shadowing correlation on wireless network performance, in: IEEE INFOCOM 2018-IEEE Conference on Computer Communications, IEEE, 2018, http://dx.doi.org/10.1109/INFOCOM.2018.8485965.

[14] T. Bai, R. Vaze, R.W. Heath, Analysis of blockage effects on urban cellular networks, IEEE Trans. Wirel. Commun. 13 (9) (2014) 5070–5083, http://dx.doi.org/10.1109/TWC.2014.2331971.